J|A|C|S
ARTICLES
Published on Web 03/26/2004

Line Narrowing in Methyl-TROSY Using Zero-Quantum ^{1}H-^{13}C NMR Spectroscopy

Vitali Tugarinov, Remco Sprangers, and Lewis E. Kay*

Contribution from the Protein Engineering Network Centers of Excellence and Departments of Medical Genetics, Biochemistry and Chemistry, The University of Toronto, Toronto, Ontario, Canada, M5S 1A8

Received November 21, 2003; E-mail: kay@pound.med.utoronto.ca

Abstract: An enhanced sensitivity zero-quantum correlation experiment is proposed for recording ^{1}H-^{13}C correlations of methyl groups in highly deuterated, methyl protonated large proteins. The zero-quantum spectra benefit from TROSY-effects in which *both* intra- and inter-methyl dipolar relaxation interactions are minimized. Applications to malate synthase G at 5 °C (81 kDa single polypeptide chain enzyme, correlation time of 118 ns) and lysine decarboxylase at 45 °C (810 kDa decameric enzyme) are presented showing significant improvements in resolution relative to corresponding HMQC data sets, with only slight decreases (∼10%) in sensitivity.

NMR spectroscopy has emerged as a powerful method for the study of molecular structure and dynamics. A major reason for the success of the technology is the relative ease of manipulation of the interactions and local fields that determine the evolution properties of the spins from which the observed signal is derived.[1] One important example of where local fields can be minimized and hence relaxation times increased is the case of TROSY of ^{1}H-^{15}N spin pairs attached to macromolecules.[2] Here the partial cancellation of fields due to the interplay between chemical shift anisotropy (CSA) and dipolar interactions leads to line narrowing, resulting in spectra with significantly improved resolution and sensitivity.[3,4] Recently we have shown that it is also possible to record TROSY-based ^{1}H-^{13}C correlation spectra of rapidly rotating methyl groups attached to large, highly deuterated proteins,[5,6] using the well-established HMQC pulse scheme.[7,8] In this experiment cancellation of intramethyl ^{1}H-^{1}H and ^{1}H-^{13}C dipolar interactions is maximized so that high quality spectra can be obtained. Contributions to relaxation from spins external to the methyl in question are minimized through the use of highly deuterated samples with protonation restricted to methyls of Ile ($\delta1$), Leu, and Val. We have recently shown that in the case of Leu and Val, far better spectra can be obtained with samples in which only one of the two methyls is of the $^{13}CH_3$ variety, with the other $^{12}CD_3$.[9]

Although deuteration does significantly improve the quality of methyl correlations in ^{1}H-^{13}C spectra, it is clear that dipolar interactions between the methyl spins and the surrounding pool of deuterons, and dilute proton spins on neighboring methyl groups, do still contribute to the relaxation of the coherences of interest. Minimization of these external fields would lead to line narrowing in spectra (relative to HMQC data sets) that might well be important in applications to high molecular weight particles where resolution is critical. Here we show that a zero-quantum (ZQ) analogue of the HMQC experiment, HZQC, provides the desired suppression, leading to noticeable improvements in spectral resolution, with only slight decreases in sensitivity. Applications to malate synthase G (MSG), an 81 kDa single polypeptide chain enzyme, and lysine decarboxylase (LDC), an 810 kDa decameric enzyme, are presented, establishing the utility of the methodology.

Materials and Methods

NMR Samples. U-[^{2}H,^{15}N] Ile$\delta1$-[$^{13}CH_3$], Leu,Val-[$^{13}CH_3$,$^{12}CD_3$] samples of MSG and protein L were prepared using D_2O-based minimal growth media and [^{12}C,^{2}H]-d-glucose as the main carbon source as described previously.[9] One hundred milligrams each of 2-keto-3,3-d_2-4-^{13}C-butyrate and 2-keto-3-methyl-d_3-3-d_1-4-^{13}C-butyrate was added to 1L growth media 1 h prior to induction, leading to the selective incorporation of $^{13}CH_3$ groups into $\delta1$ positions of Ile and selective [$^{13}CH_3$,$^{12}CD_3$] labeling of Leu/Val isopropyl moieties.[9] A U-[^{2}H,^{15}N] Ile$\delta1$-[$^{13}CH_3$] sample of LDC[10] was obtained by protein overexpression from a culture of *Escherichia coli* BL21(DE3) pLysS cells (pET3 vector) in 500 mL of D_2O M9 medium, using [^{12}C,^{2}H]-d-glucose as the main carbon source, supplemented by the addition of 40 mg of 2-keto-3,3-d_2-4-^{13}C-butyrate 1 h prior to induction. After cell-lysis in the presence of excess cofactor pyridoxal phosphate, LDC was purified to homogeneity by heating the cell supernatant to 60 °C for 8 min and applying the soluble fraction to a size-exclusion chromatography

(1) Ernst, R. R.; Bodenhausen, G.; Wokaun, A. *Principles of Nuclear Magnetic Resonance in One and Two Dimensions*; Oxford University Press: Oxford, 1987.
(2) Pervushin, K.; Riek, R.; Wider, G.; Wüthrich, K. *Proc. Natl. Acad. Sci. U.S.A.* **1997**, *94*, 12366−12371.
(3) Salzmann, M.; Pervushin, K.; Wider, G.; Senn, H.; Wüthrich, K. *Proc. Natl. Acad. Sci. U.S.A.* **1998**, *95*, 13585−13590.
(4) Yang, D.; Kay, L. E. *J. Am. Chem. Soc.* **1999**, *121*, 2571−2575.
(5) Tugarinov, V.; Hwang, P.; Ollerenshaw, J.; Kay, L. E. *J. Am. Chem. Soc.* **2003**, *125*, 10420−10428.
(6) Ollerenshaw, J. E.; Tugarinov, V.; Kay, L. E. *Magn. Reson. Chem.* **2003**, *41*, 843−852.
(7) Mueller, L. *J. Am. Chem. Soc.* **1979**, *101*, 4481−4484.
(8) Bax, A.; Griffey, R. H.; Hawkings, B. L. *J. Magn. Reson.* **1983**, *55*, 301−315.
(9) Tugarinov, V.; Kay, L. E. *J. Biomol. NMR* **2004**, *28*, 165−172.
(10) Sabo, D. L.; Boeker, E. A.; Byers, B.; Waron, H.; Fischer, E. H. *Biochemistry* **1974**, *13*, 662−670.

column. The fraction containing LDC was exchanged into 99.9% D_2O, 50 mM sodium phosphate, pH 6.8 (uncorrected), 20 mM NaCl, 3mM DTT, and concentrated to 0.8 mM in monomer (80 μM in complex). The sample of protein L was 1.2 mM in protein, 99.9% D_2O, 50 mM Na_3PO_4, pH 6.0 (uncorrected), 0.05% NaN_3 while a 1.0 mM MSG sample (99.9% D_2O, 25 mM sodium phosphate, pH 7.1 (uncorrected), 20 mM $MgCl_2$, 0.05% NaN_3, 0.1 mg/mL Pefabloc, 5 mM DTT) was employed. All biosynthetic precursors were obtained from Isotec (Miamisburg, OH) and quantitatively exchanged to ^{2}H at position 3 according to Goto et al.[11]

NMR Spectroscopy. All NMR experiments were performed on Varian Inova spectrometers equipped with pulsed-field gradient room-temperature triple resonance probes. Measurements of the relaxation rates for the slowly relaxing DQ and ZQ components (see below) were carried out at 600 and 800 MHz spectrometer fields using a pulse scheme that will be described elsewhere, with parametrically varied relaxation delays between 2 and 40(60) ms for MSG at 20(37) °C and with delays between 1 and 150 ms for protein L at 25 and 5 °C. HMQC and HZQC data sets were recorded on U-[^{2}H,^{15}N] Ileδ1-[$^{13}CH_3$], Leu,Val-[$^{13}CH_3$,$^{12}CD_3$] MSG at 5 °C, with (t_1,t_2) acquisition times of (47 ms, 64 ms), 16 scans/FID, and a 1.5 s recycle delay (net experimental time of approximately 2 h per spectrum at 600 MHz). Corresponding data sets for U-[^{2}H,^{15}N] Ileδ1-[$^{13}CH_3$] LDC were obtained at 45 °C, 800 MHz, with (t_1,t_2) acquisition times of (24 ms, 64 ms), 224 scans/FID and a recycle delay of 1.5 s, giving rise to net acquisition times of 10 hours/spectrum. All NMR spectra were processed using NMRPipe/NMRDraw software;[12] 50° shifted squared sine-bell functions in t_1 were employed for MSG, while for LDC 36° shifted sine-bell functions were used, with forward-backward linear prediction[13] in t_1 for all data sets.

Results and Discussion

Before discussing some of the important features of the ^{1}H-^{13}C zero-quantum-based experiment that partially suppresses dipolar interactions involving external spins, it is worthwhile to review very briefly some of the elements of methyl-TROSY spectroscopy, focusing on the HMQC experiment. The transfer of magnetization during this scheme can be described succinctly as $H \rightarrow H,C_{MQ}$ (t_1) $\rightarrow$ H (t_2), where H,C_{MQ} refers to the multiple-quantum coherences that evolve during t_1. It has been shown that in the macromolecular limit and assuming very fast methyl rotation, 50% of the ^{1}H transitions relax slowly (independent of intramethyl ^{1}H-^{1}H dipolar interactions) and that 50% of coherences that contribute to H,C_{MQ} relax in a manner independent of intramethyl ^{1}H-^{1}H and ^{1}H-^{13}C dipolar interactions.[5] Moreover, the flow of magnetization throughout the experiment ensures that the slowly relaxing ^{1}H signal is transferred to the slowly relaxing MQ elements and back to the slowly relaxing ^{1}H transitions for detection; a second pathway involving fast relaxing components also exists, but for applications involving large proteins, this pathway makes little or no contribution to the final signal and will be ignored in what follows. All relaxation rates discussed below refer, therefore, to those describing the decay of the slowly relaxing components. The double- (DQ) and zero-quantum (ZQ) coherences that comprise H,C_{MQ} are interconverted by a ^{1}H 180° pulse in the middle of the t_1 period so that, to excellent approximation, the effective relaxation rate during this interval is given by $(R_{DQ} + R_{ZQ})/2$, where R_{DQ} and R_{ZQ} are the relaxation rates of the ^{1}H,^{13}C DQ and ZQ coherences, respectively. In the macromolecular limit and assuming very rapid methyl rotation, these rates (R_{DQ}, R_{ZQ}) do not depend on intra-methyl dipolar interactions;[5] they are, however, influenced by external spins, with $(R_{DQ} - R_{ZQ})/2$ well approximated in the absence of chemical exchange by

$$\frac{(R_{DQ} - R_{ZQ})}{2} = \frac{16}{15}\sum_i \frac{\hbar^2\gamma_D^2\gamma_H\gamma_C S_{axis}^2\tau_c}{r_{eff,CD_i^E}^3 r_{eff,HD_i^E}^3} + \frac{2}{5}\sum_j \frac{\hbar^2\gamma_H^3\gamma_C S_{axis}^2\tau_c}{r_{eff,CH_j^E}^3 r_{eff,HH_j^E}^3} \quad (1)$$

where terms 1 and 2 account for cross-correlations between ^{13}C-^{2}H^E, ^{1}H-^{2}H^E and between ^{13}C-^{1}H^E, ^{1}H-^{1}H^E dipolar interactions, respectively, with C and H denoting methyl carbon and proton spins. In eq 1, S_{axis} is the order parameter describing the amplitude of motions of the bond connecting the methyl and its directly attached carbon, τ_C is the correlation time for overall tumbling (assumed isotropic) and $r_{eff,k}$ are effective distances between C, H and external deuterons or protons, D_i^E and H_j^E (E refers to an external spin). Factors which depend on the relative orientations of the interacting dipole vectors and contributions from methyl rotation which can modulate both the distance and angular parts of the dipolar Hamiltonian are implicitly included in $1/r_{eff,k}^3$. Equation 1 includes only terms proportional to τ_C and neglects contributions from ^{1}H CSA-^{13}C CSA cross-correlations;[14] however, such terms are small (estimated at less than 1 s^{-1} at 800 MHz for $\tau_C = 45$ ns). Expressions very similar to eq 1 have been derived previously by Konrat and Sterk[14] and Norwood[15] in the case of AX spin systems.

Figure 1a shows experimental values of $(R_{DQ} - R_{ZQ})/2$ for U-[^{2}H,^{15}N] Ileδ1-[$^{13}CH_3$], Leu,Val-[$^{13}CH_3$,$^{12}CD_3$]-labeled samples of protein L (7 kDa, 25 °C, 5 °C) and malate synthase G (MSG, 81 kDa, 37 °C, 20 °C; decay rates could not be well quantified at lower temperatures) recorded at 600 MHz using a pulse scheme in which R_{DQ} and R_{ZQ} are recorded separately. It is clear that $R_{DQ} > R_{ZQ}$, so that line narrowing can be achieved in spectra recording ZQ (decay rate R_{ZQ}) relative to MQ (effective decay rate of $0.5(R_{DQ} + R_{ZQ})$) coherences in t_1. Of note, on the basis of distances measured from the X-ray structures of protein L[16] and MSG,[17] contributions from external deuterons are estimated to make up greater than 50% of $(R_{DQ} - R_{ZQ})$ in the samples used here (dominated by intraresidue spins). Figure 1b plots histograms of $0.5(R_{DQ} + R_{ZQ})/R_{ZQ}$, obtained from measurements on MSG samples, at 600 and 800 MHz and at 37, 20 °C, corresponding to the ratio of F_1 line widths of correlations in HMQC versus HZQC data sets acquired with long t_1 acquisition times. This ratio is independent of the molecular tumbling correlation time, so long as the tumbling is in the macromolecular limit, and is also independent of spectrometer field (see eq 1) in the limit that chemical exchange effects are small. Thus, gains in resolution associated with HZQC spectra relative to HMQC data sets will be observed at any field, so

(11) Goto, N. K.; Gardner, K. H.; Mueller, G. A.; Willis, R. C.; Kay, L. E. *J. Biomol. NMR* **1999**, *13*, 369−374.
(12) Delaglio, F.; Grzesiek, S.; Vuister, G. W.; Zhu, G.; Pfeifer, J.; Bax, A. *J. Biomol. NMR* **1995**, *6*, 277−293.
(13) Zhu, G.; Bax, A. *J. Magn. Reson.* **1992**, *98*, 192−199.
(14) Konrat, R.; Sterk, H. *Chem. Phys. Lett.* **1993**, *203*, 75−80.
(15) Norwood, T. J.; Tillett, M. L.; Lian, L. Y. *Chem. Phys. Lett.* **1999**, *300*, 429−434.
(16) O'Neill, J. W.; Kim, D. E.; Baker, D.; Zhang, K. Y. J. *Acta Crystallogr., Sect. D* **2001**, *D57*, 480−487.
(17) Howard, B. R.; Endrizzi, J. A.; Remington, S. J. *Biochemistry* **2000**, *39*, 3156−68.

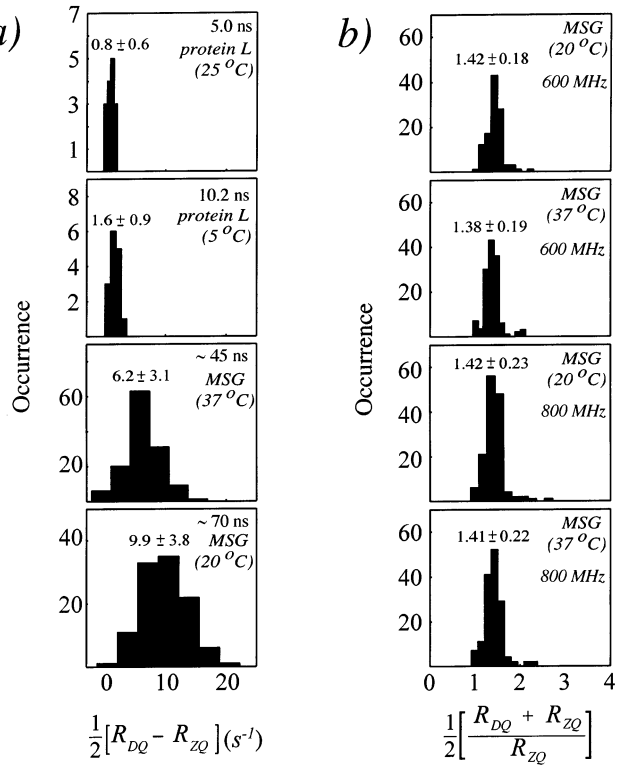

Figure 1. (a) Histograms of $(R_{DQ} - R_{ZQ})/2$ measured for protein L (top 2 panels) and MSG at different temperatures, 600 MHz; τ_c values are indicated in the top right corner of each panel. Rates have been measured for Ile, Leu, and Val methyls in U-[^{15}N,^{2}H], Ileδ1-[^{13}CH$_3$], Leu,Val-[^{13}CH$_3$,^{12}CD$_3$] protein samples. Mean values of $(R_{DQ} - R_{ZQ})/2$ (s^{-1}), along with standard deviations, are shown above each histogram. (b) Histograms of $0.5(R_{DQ} + R_{ZQ})/R_{ZQ}$ showing that in the macromolecular limit, the ratio of F_1 line widths obtained from HMQC and HZQC correlations is independent of τ_c as well as of external magnetic field (in the absence of exchange). Mean values of $0.5(R_{DQ} + R_{ZQ})/R_{ZQ}$ and associated standard deviations, are shown above each histogram. Histograms of data for protein L are based on a sample size of 15, while those for MSG are derived on the basis of data from 109 (600 MHz, 20 °C), 131 (600 MHz, 37 °C), 141 (800 MHz, 20 °C), and 150 (800 MHz, 37 °C) residues.

long as applications involve high molecular weight systems ($\omega_C\tau_C \gg 1$, where τ_C is the overall correlation time).

Figure 2 shows an enhanced sensitivity HZQC pulse sequence that has been used to record ZQ ^{1}H-^{13}C methyl correlation maps of methyl protonated, highly deuterated proteins, with both cosine and sine modulated t_1 components obtained in each scan. Quadrature detection in this scheme is achieved by alternating the position of the ^{1}H refocusing pulse between points *a* and *b*, changing the phase cycle concomitantly (see legend to Figure 2), and storing the resultant signals in separate memory locations. Thus, immediately prior to acquisition, the signal is proportional to $H_Y \cos(\omega_H\text{-}\omega_C)t_1 - H_X \sin(\omega_H\text{-}\omega_C)t_1$ (*a*) or to $H_Y \cos(\omega_H\text{-}\omega_C)t_1 + H_X \sin(\omega_H\text{-}\omega_C)t_1$ (*b*), where H_i is the *i* component of proton magnetization. Processing the data set using the enhanced sensitivity protocol[18,19] leads to correlation maps which are $\sqrt{2}$ more sensitive than schemes which record cosine and sine modulated quadrature components individually[18] since the signal intensities are doubled, while the noise floor is increased by $\sqrt{2}$. Therefore, in the absence of relaxation, only a factor of $\sqrt{2}$ in sensitivity is lost compared to the regular

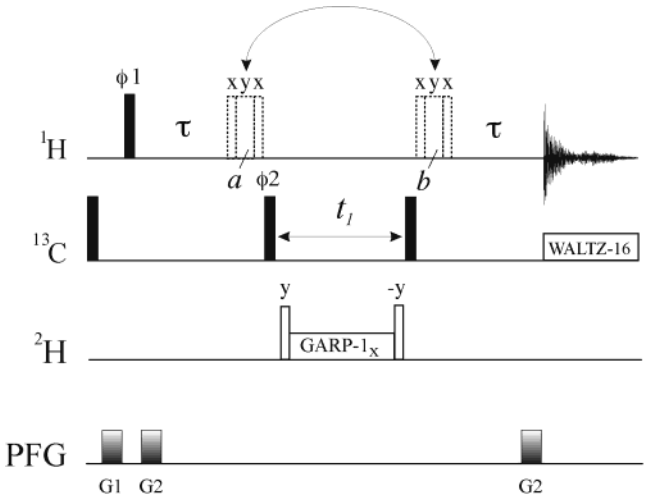

Figure 2. HZQC pulse scheme used to record high-resolution ZQ ^{1}H-^{13}C spectra of protonated methyl groups in deuterated proteins. All narrow (wide) rectangular pulses are applied with flip angles of 90° (180°) along the *x*-axis unless indicated otherwise. All ^{1}H and ^{13}C pulses are applied with the highest available power, with ^{13}C WALTZ-16 decoupling[25] achieved using a 2-3 kHz field. Two separate data sets are recorded for each t_1 point corresponding to (i) the composite ^{1}H pulse at position *a* and (ii) the composite ^{1}H pulse at position *b*. Subsequently the spectra are added and subtracted to generate sensitivity enhanced hypercomplex data as described by Kay et al.[19] The phase cycling employed is as follows: $\phi1 = x,y$; $\phi2 = x,y,-x,-y$; rec $= x,-x,-x,x$ when the ^{1}H composite pulse is applied at position *a* and rec $= x,x,-x,-x$ when it is applied at position *b*. The use of ^{2}H decoupling is optional (we have found sensitivity gains of 3−4% when it is used). ^{2}H decoupling is achieved with a 500 Hz GARP-1 field[26] flanked by 90° (2.0 kHz) ^{2}H pulses. Delay τ is set to 3.6 ms. The durations and strengths of the pulsed field gradients applied along the *z*-axis are: $g_1 =$ (1.0 ms, 7.5 G/cm), $g_2 =$ (0.5 ms, 10 G/cm).

HMQC experiment, and less when relaxation is considered (the corresponding "enhanced" HMQC experiment is not an option as it involves additional ^{1}H 90° pulses, leading to losses in sensitivity due to mixing of fast and slowly relaxing ^{1}H coherences[5]). Provided that t_1 acquisition times are sufficiently long, the lower relaxation rates of the ZQ coherences compensate for much of the $\sqrt{2}$ loss in sensitivity relative to HMQC, resulting in ZQ spectra of close to the same sensitivity and significantly better resolution than their HMQC counterparts (see below).

The Ile regions of HMQC and HZQC spectra recorded on a U-[^{2}H,^{15}N] Ileδ1-[^{13}CH$_3$], Leu,Val-[^{13}CH$_3$,^{12}CD$_3$] sample of MSG at 5 °C ($\tau_c \approx 118$ ns), 600 MHz, are compared in Figure 3a−d. As described above, the process of addition and subtraction of the enhanced sensitivity data sets leads to an increased noise floor by a factor of $\sqrt{2}$ for HZQC maps. We have therefore multiplied the HZQC data set by $1/\sqrt{2}$ so that the root-mean-squared-noise is the same in both HMQC and HZQC maps and in what follows all comparisons involve data sets with the same noise floor. In the absence of relaxation effects, correlations in the ZQ data set are expected to be $\sqrt{2}$ lower in intensity than the corresponding cross-peaks in the HMQC data set (after multiplication of the HZQC by $1/\sqrt{2}$). Figure 3a−d makes it clear, however, that the correlations in the HZQC spectrum are of comparable intensity to those in the HMQC, with an overall decrease in signal intensity of 8−12% in HZQC maps acquired with long t_1 times. The differences in R_{MQ} and R_{ZQ}, illustrated in Figure 1, explain the absence of substantial differences in signal intensities in the two data sets, Figure 3, and concomitant line narrowing (~30% of the HMQC line width).

(18) Cavanagh, J.; Rance, M. *Ann. Rep. NMR Spectrosc.* **1993**, *27*, 1−58.
(19) Kay, L. E.; Keifer, P.; Saarinen, T. *J. Am. Chem. Soc.* **1992**, *114*, 10663−10665.

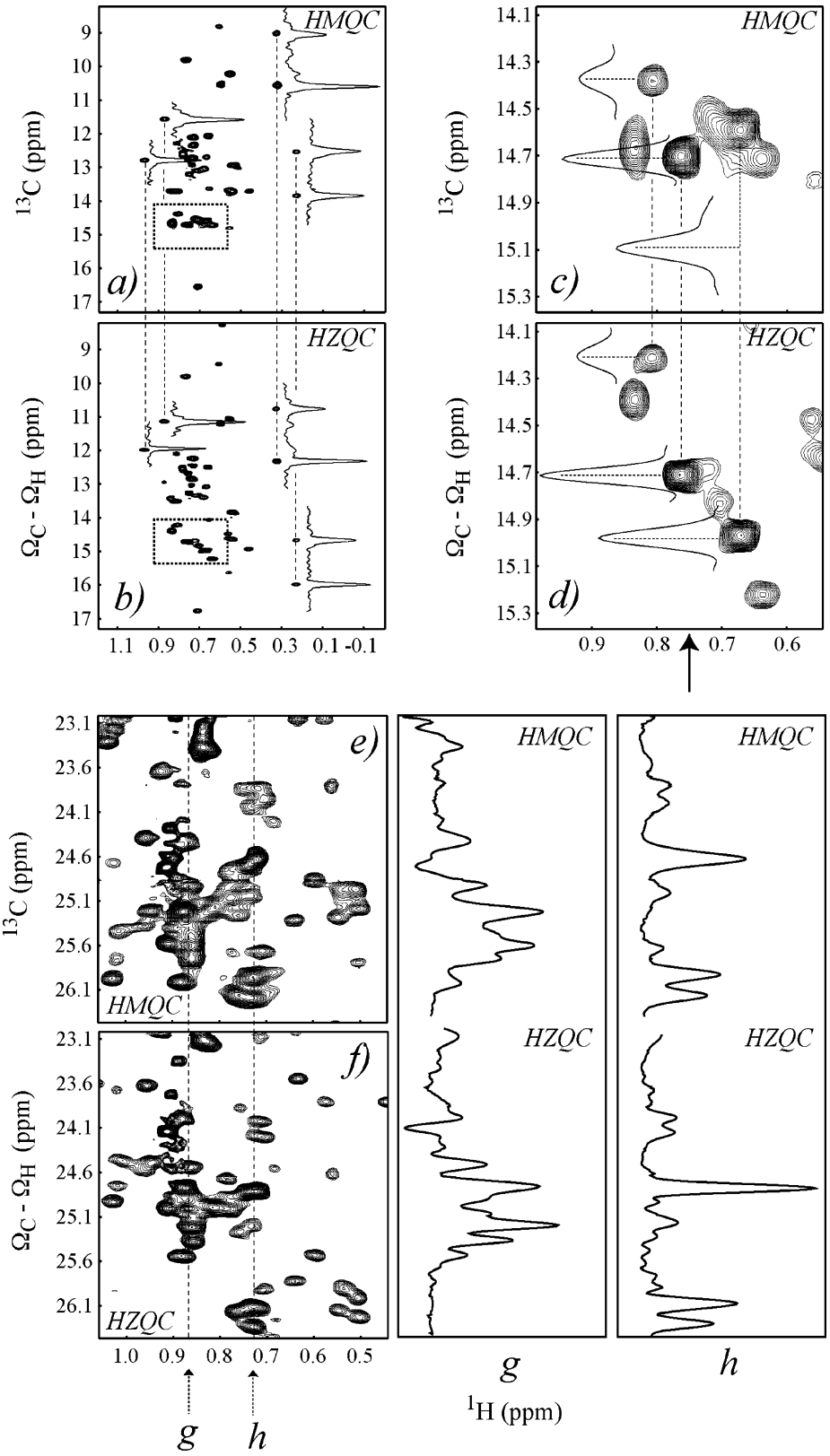

Figure 3. (a−d) Comparison of the Ile regions of high-resolution ^{1}H-^{13}C HMQC (a) and HZQC (b) correlation maps recorded on a U-[^{15}N,^{2}H] Ileδ1-[$^{13}CH_3$], Leu,Val-[$^{13}CH_3$,$^{12}CD_3$] sample of MSG (81 kDa) at 5 °C (600 MHz). The spectra were processed identically and are displayed at the same contour levels; the noise floor in each data set is the same, see text. The region enclosed in dashed boxes in panels a and b is shown in panels c and d for HMQC and HZQC spectra, respectively. Dashed vertical lines connect the peaks corresponding to the same methyl groups in the HMQC and HZQC spectra. Correlations in HZQC spectra are located in F_1 at the differences of ^{1}H and ^{13}C shifts (Hz) from their respective carriers. For simplicity we have labeled the axis exactly as was done for the HMQC data set. The position of the carrier in the direct ^{1}H dimension (0.76 ppm) is shown with an arrow below panel d. (e−h) Comparison of Leu/Val regions of ^{1}H-^{13}C HMQC and HZQC correlation maps (same data set as for Ile above). Contours are plotted at the same levels in HMQC and HZQC spectra and both data sets have the same noise floor. Cross-sections at points g, and h are shown in the two panels to the right of the spectra.

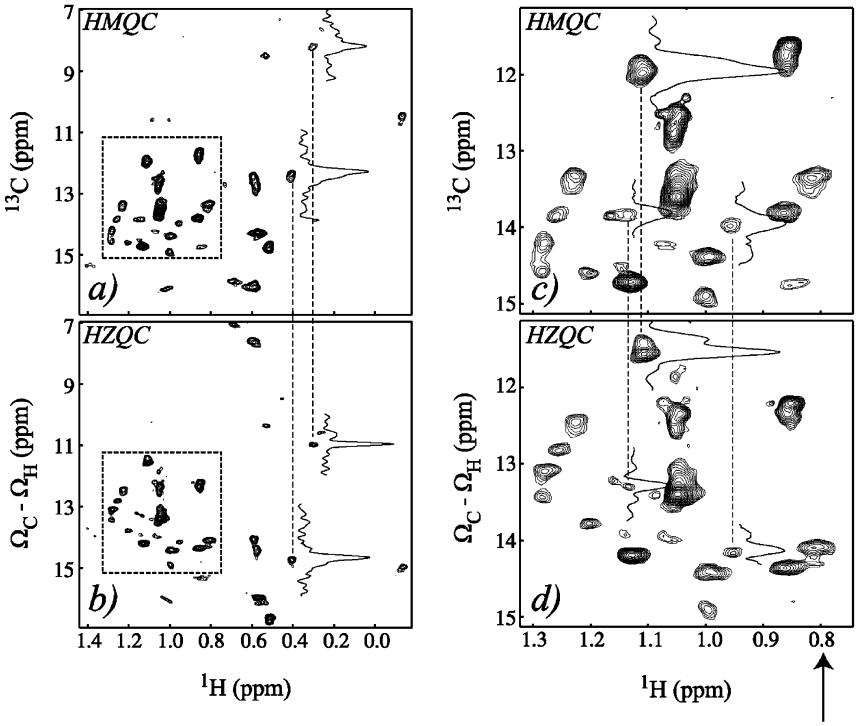

Figure 4. (a−d) Comparison of high-resolution ^{1}H-^{13}C HMQC (a) and HZQC (b) maps recorded on a U-[^{15}N,^{2}H], Ileδ1-[^{13}CH$_3$] sample of LDC (810 kDa) at 45 °C (800 MHz). Both data sets have the same noise floor (see text) and are plotted with the same contour levels. S/N is approximately 10% lower in the HZQC data set, and not the 30% that would be expected in the absence of differential relaxation of ZQ and MQ coherences. The position of the ^{1}H carrier (0.8 ppm) is indicated by the vertical arrow below panel d.

Figure 3e−h shows the Leu,Val regions from the same set of spectra illustrated in Figure 3a−d, establishing that similar gains in resolution and small losses in sensitivity (∼10%) are observed for Leu and Val methyls as well. It is noteworthy that the gains in resolution obtained at 600 MHz have also been observed in spectra recorded at 800 MHz, as expected from Figure 1b.

Figure 4 compares HMQC and HZQC spectra recorded on a U-[^{2}H,^{15}N] Ileδ1-[^{13}CH$_3$], 810 kDa decamer, LDC, at 45 °C, 800 MHz. On the basis of electron microscopy of LDC[10] and X-ray studies of a homologue,[20] ornithine decarboxylase, it is expected that the 10 monomers of LDC are equivalent, with 49 Ile/monomer. Conservatively, approximately 40 peaks can be quantified in HZQC/HMQC spectra, and the ZQ data set is only slightly lower in signal-to-noise (S/N) with relative S/N values of 0.94 ± 0.22 (0.22 is the standard deviation of the S/N among the quantified peaks). Although there is a significant decrease in absolute sensitivity of these data sets in relation to the corresponding spectra recorded on MSG, it is clear that resolution gains are obtained in ZQ maps for this system as well.

As described above, the gains in resolution in HZQC spectra relative to HMQC (or double-quantum data sets for that matter) are a direct consequence of the fact that external spins (i.e., those spins outside of the methyl group in question) relax ^{1}H,^{13}C DQ coherences more efficiently than the corresponding ZQ elements, eq 1 ($R_{DQ} - R_{ZQ} > 0$). It is also the case that $|R_{DQ} - R_{ZQ}| > 0$ when relaxation is dominated by chemical exchange. Unlike the situation involving dipolar relaxation described here, however, ($R_{DQ} - R_{ZQ}$) can be either positive or negative when exchange is the main source of relaxation.[21−23] This implies that exchange contributions can at least be partially suppressed in one of either double- or zero- quantum correlation maps, although a priori it is not possible to predict in which one for a given exchanging resonance. By recording both DQ/ZQ data sets, however, correlations with significantly improved intensity can be obtained in one of the spectra, demonstrated recently by Pervushin.[24]

In summary, we have described a ZQ methyl-TROSY experiment that protects against intra-methyl dipolar interactions in a manner similar to the HMQC scheme and, in addition, minimizes contributions from relaxation interactions involving external ^{1}H or ^{2}H spins in highly deuterated, methyl protonated large proteins. The line narrowing observed in the HZQC experiment relative to the HMQC scheme more than compensates for the marginal reduction in sensitivity, especially for applications to high molecular weight particles where resolution considerations are critical.

Acknowledgment. This work was supported by a grant from the Canadian Institutes of Health Research to L.E.K. V.T. and R.S. acknowledge the support of the Human Frontiers Science Program and the Netherlands Organization for Scientific Research, respectively. The authors are grateful to Professor Walid Houry, University of Toronto, for the gift of the LDC plasmid. L.E.K. holds a Canada Research Chair in Biochemistry.

JA039732S

(20) Momany, C.; Ernst, S.; Ghosh, R.; Chang, N. L.; Hackert, M. L. *J. Mol. Biol.* **1995**, *252*, 643−655.

(21) Kloiber, K.; Konrat, R. *J. Biomol. NMR* **2000**, *18*, 33−42.
(22) Fruh, D.; Tolman, J. R.; Bodenhausen, G.; Zwahlen, C. *J. Am. Chem. Soc.* **2001**, *123*, 4810−4816.
(23) Wang, C. Y.; Palmer, A. G. *J. Biomol. NMR* **2003**, *24*, 263−268.
(24) Pervushin, K. *J. Biomol. NMR* **2001**, *20*, 275−285.
(25) Shaka, A. J.; Keeler, J.; Frenkiel, T.; Freeman, R. *J. Magn. Reson.* **1983**, *52*, 335−338.
(26) Shaka, A. J.; Barker, P. B.; Freeman, R. *J. Magn. Reson.* **1985**, *64*, 547−552.